
OAo/MITSuME Photometry of Dwarf Novae. III. CSS130418:174033+414756

Akira IMADA,^{1,2*} Keisuke ISOGAI,³ Kenshi YANAGISAWA,⁴ Nobuyuki KAWAI⁵

¹Hamburger Sternwarte, Universität Hamburg, Gojenbergsweg 112, D-21029 Hamburg, Germany

²Kwasan and Hida Observatories, Kyoto University, Yamashina, Kyoto 607-8471, Japan

³Department of Astronomy, Kyoto University, Kyoto 606-8502, Japan

⁴Okayama Astrophysical Observatory, National Astronomical Observatory of Japan, Asakuchi, Okayama 719-0232, Japan

⁵Department of Physics, Tokyo Institute of Technology, Ookayama 2-12-1, Meguro-ku, Tokyo 152-8551, Japan

*E-mail: *a_imada@kusastro.kyoto-u.ac.jp

Received 201 0; Accepted 201 0

Abstract

We report on multicolour photometry of the short period dwarf nova CSS130418:174033+414756 during the 2013 superoutburst. The system showed an unusually short superhump period with 0.046346(67) d during stage A, which is one of the shortest periods among dwarf novae below the period minimum. We found that the bluest peaks in $g' - I_c$ colour variations tend to coincide with the brightness minima of the superhump modulations. We also studied nightly-averaged superhump amplitudes in g' , R_c , and I_c bands and found that they have less dependence on wavelength. These properties are likely to be in common with dwarf novae exhibiting superhumps. We successfully obtained $g' - R_c$ and $R_c - I_c$ colours during the temporal dip. The colour indices were significantly bluer compared with other dips of WZ Sge-type dwarf novae. By using the period of the growing superhumps, we estimated the mass ratio to be $q = 0.077(5)$, which is much larger than the previous study.

Key words: accretion, accretion discs — stars: dwarf novae — stars: individual (CSS130418:174033+414756) — stars: novae, cataclysmic variables — stars: oscillations

1 Introduction

Cataclysmic variables (CVs) are close binary stars that consist of a primary white dwarf and a secondary star. The secondary star fills its Roche lobe, transferring gas into the primary Roche lobe through the inner Lagrangian point (L1). As a result, an accretion disc is formed around the white dwarf if the magnetic field of the white dwarf is sufficiently weak (for a review, see, e.g., Warner 1995; Hellier 2001).

CVs are divided into several subclasses according to the overall light curves and underlying physics causing the variations. Dwarf novae are a subclass of CVs. They

exhibit outbursts with recurrent time scales of days to years with amplitudes of 2–8 mag (for a review, see, e.g., Osaki 1996; Lasota 2001). The overall behaviour of dwarf novae is well explained by the thermal limit cycle-instability model of the accretion disc (Meyer, Meyer-Hofmeister 1981; Smak 1984).

Dwarf novae are further divided into several subclasses with respect to their light curves (Kato et al. 2004b; Kato et al. 2009). SU UMa-type dwarf novae, one subclass of dwarf novae, show two types of outbursts. One is called normal outburst, whose duration is a few days, and the other is called superoutburst, whose duration is typ-

ically 2 weeks or sometimes longer and the amplitude is about 1 mag larger than the normal outburst. During the superoutburst, a rapid rise and slow decline modulations, termed superhumps, are observed. The period of the superhump (P_{sh}) is slightly longer than the orbital period of the system (P_{orb}). Long-term light curves of SU UMa-type dwarf novae are well reproduced by the combination of the thermal and tidal instability model (Osaki 1989; Osaki, Kato 2013a). The light curves of superhumps are understood as tidal dissipation of the eccentricity-deformed precessing accretion disc (Whitehurst 1988; Hirose, Osaki 1990).

Recent extensive photometry during superoutbursts has revealed that the light curves of SU UMa-type dwarf novae show a wide variety (e.g., Kato et al. 2009). WZ Sge-type dwarf novae, one subclass of SU UMa-type dwarf novae, are one of the most important systems among them, in terms of researching for various physics of the accretion discs, as well as inspection of evolutionary theories of CVs driven by the gravitational wave radiation (Kato 2015). The main characteristics of WZ Sge-type dwarf novae is that (1) they have a long quiescence, typically exceeding a decade (Nogami et al. 1997; Kato et al. 2001) (2) the maximum magnitude of the superoutburst is more than 6 mag brighter than the quiescent magnitude (Howell et al. 1995; Ishioka et al. 2001), (3) an early stage of the superoutburst show double-peaked modulations called early superhumps (Osaki, Meyer 2002; Kato 2002), (4) some of them show rebrightening(s) after the end of the superoutburst plateau (Patterson et al. 2002; Kato et al. 2004a), and (5) they are absent of normal outbursts (For a review, see Kato 2015).

It is well known that the period of superhumps changes over the course of the superoutburst (Kato et al. 2009). Our understanding of the superhump period change has been significantly improved over the past decade, mainly by statistical studies of superhumps conducted by VSNET (Kato et al. 2004b). VSNET (= Variable Star NETWORK) is a world-wide amateur-professional network of researchers in variable stars, particularly in transient objects such as cataclysmic variables (Kato et al. 2009), black-hole binaries (Kimura et al. 2016a), supernovae (Okuyudo et al. 1993), and gamma-ray bursts (Uemura et al. 2003).¹ According to Kato et al. (2009), the evolution of the superhump period consists of three stages: an early stage with a longer and constant period (stage A), a middle stage with positive $P_{dot} = \dot{P}/P$ (stage B), and a late stage with a shorter and constant period (stage C). Although the underlying physics in each stage is not clear, it has been gradually accepted that stage A

superhump period is associated with the dynamical precession rate at the 3:1 resonance radius, based on the observations of eclipsing SU UMa-type dwarf novae (Osaki, Kato 2013b; Kato, Osaki 2013).

Although extensive light curves of superoutbursts have been acquired, the majority of CCD photometry were performed without filters. Recent multicolour observations during superoutbursts have revealed a wide variety of colour variations. For example, Uemura et al. (2008) performed simultaneous optical and near-infrared observations of a WZ Sge-type dwarf nova IK Leo during the 2006 superoutburst and found a significant K_s excess during the rebrightening. Uemura et al. (2008) noted that the near-infrared activities provide evidence for the presence of mass reservoir at the outer region of the accretion disc. Matsui et al. (2009) performed multicolour observations during the 2007 superoutburst of V455 And, in which they found that the bluest peak of colour variations of superhumps are prior to their maximum brightness by a phase of 0.15. Regarding the underlying mechanism of colour variations, Matsui et al. (2009) suggested that the emitting size of the superhump light source changes as a result of viscous heating and cooling of the accretion disc, which may be observed as the difference in the maximum phase between the magnitude and colour. On the other hand, Isogai et al. (2015) found that the bluest peak of $g' - i'$ colour correspond to the brightness minimum of superhumps during the 2010 superoutburst of EZ Lyn. Similar results were obtained in the WZ Sge-type dwarf novae HV Vir, OT J012059.6+325545, and SSS J122221.7–311525 (Nakagawa et al. 2013; Neustroev et al. 2017; Imada et al. 2018). Isogai et al. (2015) noted that the different results between V455 And and EZ Lyn may be caused by the different disc radius between them, based on their photometric and spectroscopic observations. Neustroev et al. (2017) studied a relation between superhumps and colour variations according to each superhump stage and found that stage A superhumps showed weaker colour variations compared with stage B ones. Imada et al. (2018) suggest that drastic colour variations during stage B may attribute to the predominance of the pressure effect. Regarding the post-superoutburst stage, Neustroev et al. (2017) found that the superhump maxima coincide with the bluest peak of $B - I$ colour variations. In order to quantitatively study the colour variations of superhumps, further multicolour photometry is indispensable.

Recent studies have shown that the histogram of the orbital period distribution of dwarf novae has a cutoff around 78 min, below which dwarf novae hardly exists (Gänsicke et al. 2009; Uemura et al. 2010; Knigge et al.

¹ www.kusastro.kyoto-u.ac.jp/vsnet

2011). Nevertheless, several systems indeed have their orbital periods far below 78 min (Breedt et al. 2012). Such systems include e.g., V485 Cen (Augusteijn et al. 1993; Olech 1997), EI Psc (Wei et al. 2001; Thorstensen et al. 2002; Uemura et al. 2002), SBS 1108+574 (Carter et al. 2013; Littlefield et al. 2013; Kennedy et al. 2015), and OV Boo (Szkody et al. 2005; Littlefair et al. 2007; Patterson et al. 2008). Theoretical studies suggest that dwarf novae can evolve below the period minimum if the system contains an evolved secondary (Podsiadlowski et al. 2003). Such systems can provide evidence for helium enrichment in their spectra (Thorstensen et al. 2002), together with N-enhanced and C-depleted features (Gänsicke et al. 2003).

On 2013 April 18.46, Catalina Real Transient Survey (CRTS, Drake et al. 2009) detected an eruptive object (CSS130418:174033+414756, hereafter, CSS J1740) with the magnitude of ~ 14 . The All Sky Automated Survey for SuperNovae (ASAS-SN, Shappee et al. 2014) also detected the outburst on 2013 April 19.53 with $V = 12.7$ (Prieto et al. 2013). It turned out that the eruption was a superoutburst of a dwarf nova ([vsnet-alert 15639]). Surprisingly, the system showed an unusually short early superhump period with 0.04503(1) ([vsnet-alert 15639]), which is far below the observational period minimum. After this report, we started simultaneous g' , R_c , and I_c photometry using the MITSuME telescope located in the Okayama Astrophysical Observatory (OAO).² This system underwent further outbursts in 2007 May and 2014 August ([vsnet-alert 17610]). Here we report on multicolour photometry and analyses during the 2013 superoutburst of CSS J1740.

2 Observations

Time-resolved CCD photometry was performed from 2013 April 26 to 2013 May 23 using MITSuME 50cm-telescope located in Okayama Astrophysical Observatory (OAO). MITSuME 50cm-telescope is a robotic telescope that can acquire g' , R_c , and I_c images simultaneously by using two dichroic mirrors and three CCD cameras, which allows us to study colour variations of variable stars (For a detail description, see Kotani et al. 2005). We list the log of our observations in table 1. All data were obtained with the exposure time of 30 sec. The total data-points of our observations amount to 6524, which is sufficient for period and colour studies of the superoutburst.

After de-biasing, dark-subtracting and flat-fielding the images with the standard procedure, the data were processed with aperture photometry using IRAF/daophot.³

² www.oao.nao.ac.jp

³ IRAF (Image Reduction and Analysis Facility) is distributed by the National

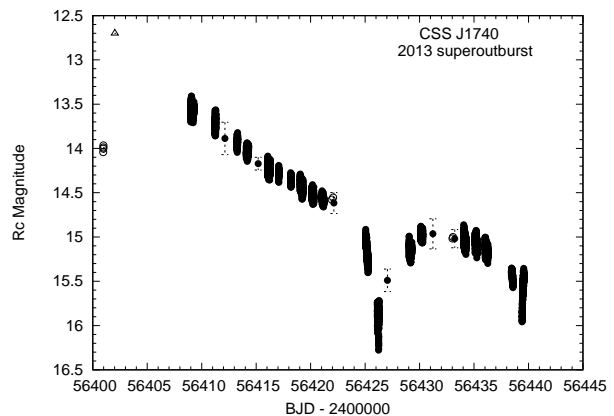


Fig. 1. The light curve of the 2013 superoutburst of CSS J1740. The abscissa denotes BJD - 2400000, while the ordinate denotes R_c magnitude. We also plot V band data of the CRTS (open circles), the ASAS-SN (open triangle), and a part of the AAVSO archival light curve (on BJD 2456438-39). A temporal dip was observed on BJD 2456425, after which the light curve showed a long-lasting rebrightening. A short-term rebrightening was caught on BJD 2455639.

We performed differential photometry using the star with RA 17:40:11.00, Dec +41:48:18.22, $g' = 12.47(6)$, $r' = 12.25(2)$, and $i' = 12.17(3)$. The constancy of the comparison star is checked by nearby stars in the same field. Because the exact magnitudes of R_c and I_c of the comparison star are unknown, we converted the SDSS magnitudes to R_c and I_c given by Smith et al. (2002) as follows:

$$V = g' - 0.55(g' - r') - 0.03 \quad (1)$$

$$V - R = 0.59(g' - r') + 0.11 \quad (2)$$

$$R - I = 1.00(r' - i') + 0.21 \quad (3)$$

Using the above equations, we adopt $g' = 12.467(37)$, $R_c = 12.077(30)$, and $I_c = 11.793(37)$ as the magnitudes of the comparison star. Barycentric correction was made before the following analyses.

3 Results and Discussion

3.1 Light curve

Figure 1 shows R_c light curve of our observations. Also shown are V band data obtained with the CRTS, ASAS-SN and a part of the AAVSO archive.⁴ In combination with our data and the initial detection by the CRTS and ASAS-SN, the plateau stage lasted for ~ 23 d. On BJD 2456425, the light curve entered a rapid fading stage and showed a temporal dip on BJD 2456426 with the magnitude faded by ~ 1.5 mag with the duration as short as 1

Optical Astronomy Observatories, which is operated by the Association of Universities for Research in Astronomy, Inc., under cooperative agreement with National Science Foundation.

⁴ <https://www.aavso.org/data-download>

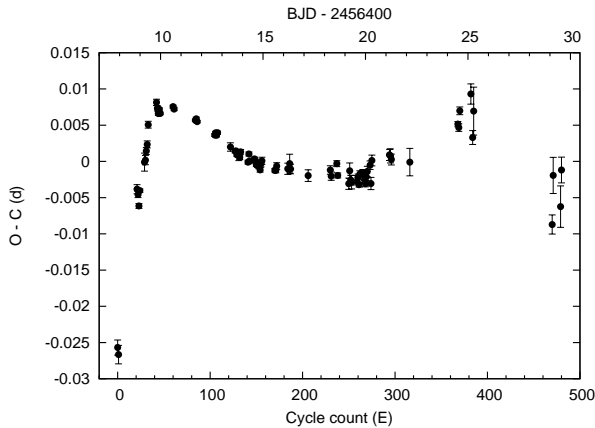


Fig. 2. $O - C$ diagram of superhump maxima. We used table 2 and equation (4) to draw the diagram. Stage A can be clearly recognized between BJD 2456408–09. This diagram also indicates that the stage B-C transition occurred on BJD 2456425.

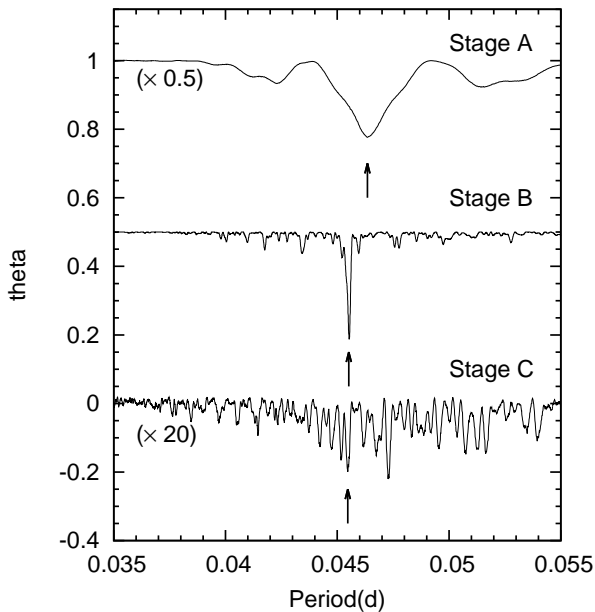


Fig. 3. Theta diagrams of each stage. The best estimated periods were 0.046346(67) d (stage A), 0.045515(29) d (stage B), and 0.045473(25) d (stage C), respectively, which are marked with the arrows. For better visualization, the theta diagrams of stage A and stage C are changed from the original sizes.

Table 1. Log of observations of CSS J1740 using MITSuME telescope.

Date	BJD(start)*	BJD(end)*	N^\dagger
2013 Apr. 26	56408.9927	56409.3060	589
2013 Apr. 28	56411.2084	56411.3055	138
2013 Apr. 29	56412.1268	56412.1340	10
2013 Apr. 30	56413.2322	56413.3033	161
2013 May. 1	56414.0946	56414.3035	389
2013 May. 2	56415.1750	56415.1842	16
2013 May. 3	56416.0347	56416.3020	423
2013 May. 4	56417.0550	56417.0942	88
2013 May. 5	56418.1552	56418.2397	182
2013 May. 6	56419.0304	56419.2997	530
2013 May. 7	56420.1013	56420.2983	361
2013 May. 8	56421.0425	56421.2169	340
2013 May. 9	56422.0385	56422.2542	304
2013 May. 12	56425.0514	56425.2945	427
2013 May. 13	56426.1250	56426.2916	304
2013 May. 14	56427.0457	56427.0554	21
2013 May. 16	56429.0365	56429.2921	474
2013 May. 17	56430.0848	56430.2928	385
2013 May. 18	56431.1932	56431.2931	17
2013 May. 20	56433.1922	56433.2626	91
2013 May. 21	56434.0436	56434.2907	454
2013 May. 22	56435.0930	56435.2924	345
2013 May. 23	56436.0103	56436.2882	475

*BJD–2400000 † Number of exposure.

d. Such a dip is remarkably similar to that observed in a well-known WZ Sge-type dwarf nova AL Com (Nogami et al. 1997; Kimura et al. 2016b). On BJD 2456427, the magnitude quickly recovered from the dip and CSS J1740 entered a long-lasting rebrightening stage. The profile of the light curve during the rebrightening stage is characteristic of type-A one introduced by Imada et al. (2006) and Kato (2015). On BJD 2456438, CSS J1740 faded rapidly with a rate of 0.94(5) mag/d, after which a short rising was observed on BJD 2456439 with a rate of $-2.58(7)$ mag/d. This is a rare phenomenon for type-A rebrightenings, but a similar light curve was observed during the 2015 superoutburst of the short-period WZ Sge-type dwarf nova ASASSN-15po (Namekata et al. 2017).

3.2 Superhump period

The superhump maxima are listed in table 2. In order to improve our period analyses, we downloaded the AAVSO light curve and combined these with our data. A linear regression to the superhump maxima yields

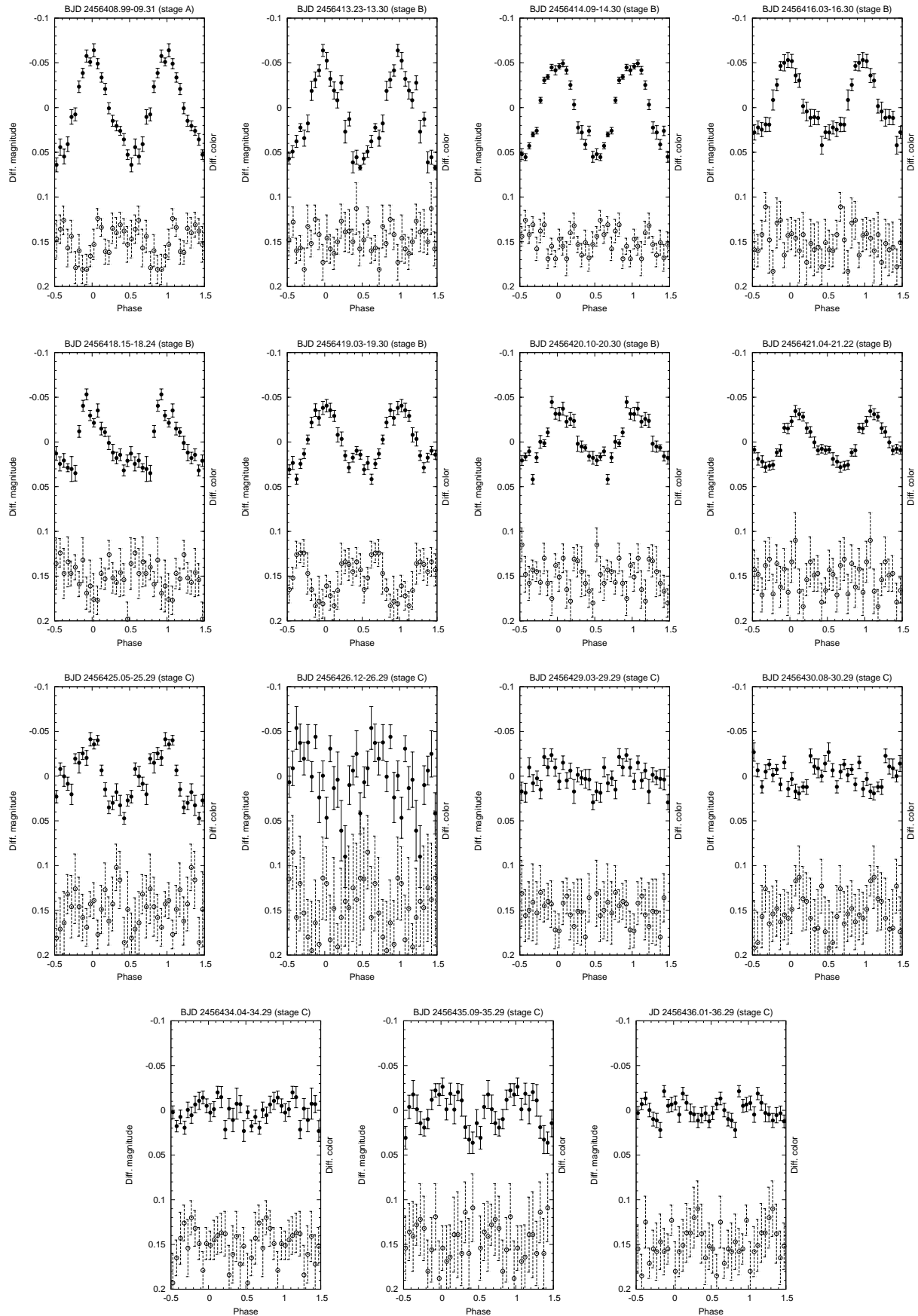


Fig. 4. Nightly-averaged R_c light curves (filled circles) and $g' - I_c$ colour variations (open circles) folded with 0.046346 d (stage A), 0.045515 d (stage B), and 0.045473 d (stage C). Single-peaked profiles, characteristic of superhumps, are visible, particularly during the plateau stage. Weak modulations are also visible during the rebrightening stage. There is a hint that the bluest peaks in $g' - I_c$ correspond to the brightness minima in some nights.

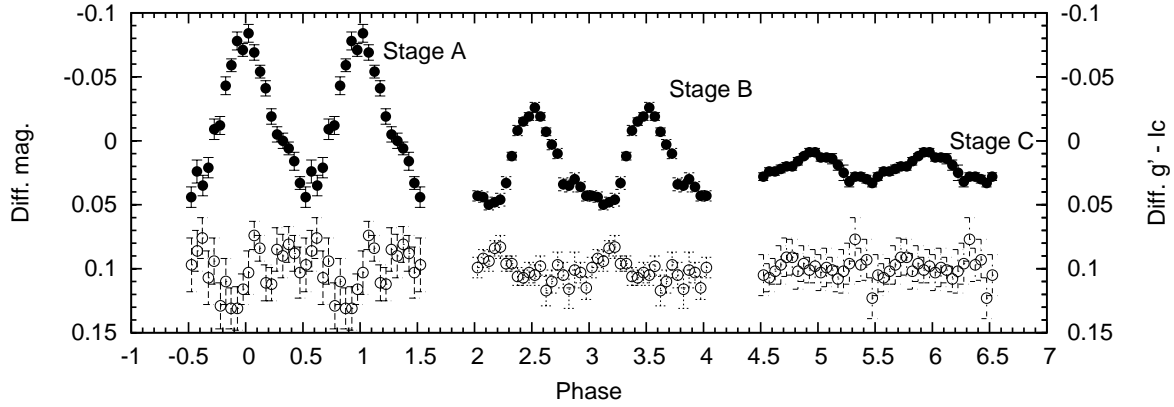


Fig. 5. R_c light curves (filled circles) and $g' - I_c$ colour variations (open circles) in each stage folded with 0.046346 d (stage A), 0.045515 d (stage B), and 0.045473 d (stage C). R_c light curve is anticorrelated with $g' - I_c$ colour variations in stage B. In common, the brightness maxima differ from the bluest peaks in $g' - I_c$ colours.

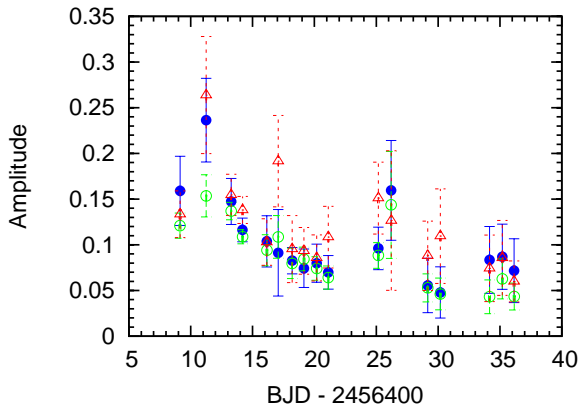


Fig. 6. Nightly-averaged superhump amplitudes in g' (filled circles, blue), R_c (open circles, green), and I_c (open triangles, red) bands. The maximum amplitudes occurred on BJD 2456411, corresponding to the beginning of stage B. A regrowth of the superhump amplitudes was observed on BJD 2456425, corresponding to the stage B–C transition.

$$BJD(max) = 2456407.6914(11) + 0.045549(5) \times E. \quad (4)$$

Based on this equation, we obtained the $O - C$ diagram of superhump maxima, which is shown in figure 2. As can be seen in the $O - C$ diagram, stage A can be clearly recognized in the early stage of our data. The obtained $O - C$ diagram indicates that stage A ended before BJD 2456409.6 ($E = 42$). We performed the Phase Dispersion Minimization method (PDM, Stellingwerf (1978)) for stage A superhumps and estimated the mean period as $P = 0.046346(67)$ d. The resultant theta diagram is displayed in the top of figure 3. The errors in the PDM method are calculated using Lafter-Kinmann class method developed by Fernie (1989) and Kato et al. (2010).

The $O - C$ diagram also shows that J1740 experienced the stage B–C transition on BJD 2456425. Based on the

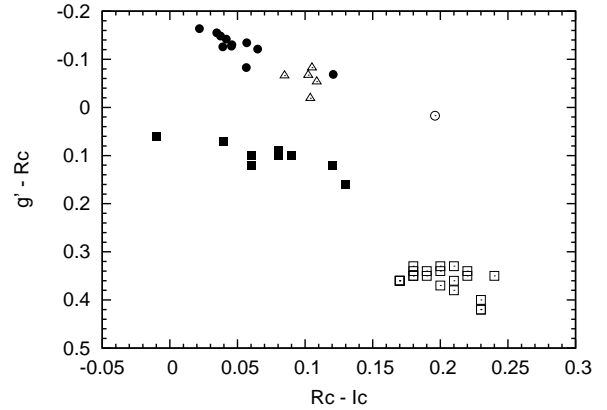


Fig. 7. Nightly-averaged colour-colour diagram of the superoutburst. The filled circles, open circle, and open triangles indicate the datapoints of the plateau stage, dip, and rebrightening stages of CSS J1740, respectively. The filled and open squares denote the datapoints of the plateau and post-superoutburst stages during the 2007 superoutburst of V455 And. Note that CSS J1740 shows bluer $g' - R_c$ colour variations compared with V455 And and the dip of CSS J1740 has a similar $R_c - I_c$ colour to the post-superoutburst stage of V455 And.

above analyses, we performed the PDM for stage B (BJD 2456409.60–24.58) and stage C (after BJD 2456425.05), and obtained the best estimated periods to be $P = 0.045515(29)$ d for stage B and $P = 0.045473(25)$ d for stage C, respectively. The resultant theta diagrams are displayed in the middle and bottom of figure 3. These obtained values are in agreement with that derived by Chochol et al. (2015) and Kato et al. (2015). The profile of the $O - C$ diagram means the positive P_{dot} during stage B. By fitting the data between $42 \leq E \leq 370$ with a quadratic equation, we obtained P_{dot} to be 1.6×10^{-5} , in good agreement with that derived by Kato et al. (2015).

3.3 Superhumps and colour variations

Figure 4 exhibits nightly-averaged R_c light curves and $g' - I_c$ colours folded with the above obtained periods. Single-peaked profiles characteristic of superhumps are visible, particularly in the early datasets of our run. Although the profiles became complicated during the rebrightening, hump-like modulations were visible. As for $g' - I_c$ colour variations, the bluest peaks tend to coincide with the brightness minima. This tendency is also reported in other WZ Sge-type dwarf novae, such as EZ Lyn (Isogai et al. 2015), SSS J122221.7–311525 (Neustroev et al. 2017), HV Vir, and OT J012059.6+325545 (Imada et al. 2018).

In order to further study the relation between the superhump and colour variations and compare our data with the previous works, we made phase-averaged R_c light curves and $g' - I_c$ colour variations in each stage, which are represented in figure 5. As noted above, the light minima of superhumps coincide with bluest peaks of $g' - I_c$ during stage A and B. There shows a common property that the brightness maximum of superhumps differ from the bluest peak of $g' - I_c$ in phase. In recent years, Isogai et al. (2015) discussed the values of the phase difference, by using the data of EZ Lyn and V455 And. The phase difference between the superhump light and colour variation was ~ 0.5 in EZ Lyn, while that was only ~ 0.15 in V455 And (see figure 8 of Matsui et al. (2009)). In the case of CSS J1740, we found ~ 0.5 in stage A and 0.3 in stage B, respectively. At present, we cannot draw a firm conclusion to the working mechanism of the phase difference, because of the lack of multicolour photometry during superoutbursts. Here we summarize the values of the phase difference in table 3. The physical mechanisms of the phase difference should be clarified by collecting further observational samples.

3.4 Amplitudes of superhumps

Figure 6 shows nightly-averaged amplitudes of superhumps in each band. Statistical studies of amplitudes of superhumps have shown that the maximum amplitude of superhumps occurs around the stage A-B transition, and that a regrowth of superhumps occurs around the stage B-C transition (Kato et al. 2009). As can be seen in this figure, the superhump amplitudes showed the largest values on BJD 2456411, corresponding to the beginning of stage B. A regrowth of the superhumps was also detected on BJD 2456425, corresponding to the beginning of stage C. Judging from these observations, the amplitude development observed in CSS J1740 is common for SU UMA-type dwarf novae.

Recently, Imada et al. (2018) reported that the amplitudes of superhumps are likely to be independent of wavelength while those of early superhumps are strongly dependent on wavelength. Although we can find a weak tendency that the I_c band has the large amplitudes in stage B and R_c band has the small amplitudes in stage C in some nights, these tendencies are not evident compared with that observed in early superhumps in WZ Sge-type dwarf novae (Imada et al. 2018).

3.5 Colour-colour diagram

In order to study colour development during the superoutburst of CSS J1740, we derived the nightly-averaged colour-colour diagram, which is displayed in figure 7. Also shown are the nightly-averaged colours during the 2007 superoutburst of V455 And, taken from table 2 of Matsui et al. (2009). At the onset of our observations, the colours of CSS J1740 were located on the top-left region in figure 7, after which the colours became red as the superoutburst proceeded. The colours during the dip significantly deviated from the majority of the datapoints. During the rebrightening stage, the colours were clustered around $g' - R_c \sim -0.05$ and $R_c - I_c \sim 0.1$. We also found that $g' - R_c$ colours during the plateau stage of CSS J1740 were about 0.2 mag bluer than those of V455 And, while the $R_c - I_c$ colours were almost the same between these systems. Because we have fewer samples of the colour-colour diagram during superoutbursts, it is unknown whether CSS J1740 shows bluer $g' - R_c$ colour variations than other systems. The textbook colour-colour diagram of superoutbursts should be established. Regarding the optical spectrum, Chochol et al. (2015) reported that CSS J1740 provides evidence for overabundance in helium. This feature is similar to that of the helium-rich dwarf nova SBS J1108+574 (Littlefield et al. 2013), although helium lines in CSS J1740 are not so strong as in SBS J1108+574. At present, it is unclear whether colour variations of J1740 are affected by a richness in helium, which should be elucidated in future multicolour photometry of various types of dwarf novae.

We also note that the colours of the dip show unique values compared with those of other stages. The dip datapoint of CSS J1740 means that $R_c - I_c$ colour already returns to the quiescent level, while $g' - R_c$ colour remains relatively blue. In order to compare our results with other observations during the dip, we estimated $g' - R_c$ and $R_c - I_c$ colours of the dips during the 1996-97 superoutburst of EG Cnc and 2001 superoutburst of WZ Sge itself. These data were taken from table 2 of Patterson et al. (1998) and table 2 of Howell et al. (2004), and we

converted these data to $g' - R_c$ by using the equation (1) and (2). Table 4 shows the resultant colours during the dip. The table clearly shows the red colours of the dips for EG Cnc and WZ Sge, while those of CSS J1740 were significantly bluer compared with those of EG Cnc and WZ Sge. Whether or not the blue dip of CSS J1740 is associated with the helium richness should be clarified in further photometric samples during the dip.

3.6 Mass ratio of CSS J1740

In recent years, Kato, Osaki (2013) have proposed a new method of estimating the mass ratio of the system using the orbital and stage A superhump periods (stage A method). This method is powerful for WZ Sge-type dwarf novae, since the observed early superhump period can be regarded as the orbital period of the system. In addition, Kato (2015) has shown that the duration of stage A superhumps tend to be inversely proportional to the mass ratio, which enables us to precisely determine the period of stage A superhumps. Although the late start of our observations prevented us from detecting early superhumps, Chochol et al. (2015) reported that the orbital period of CSS J1740 to be $P_{\text{orb}} = 0.045028(7)$ d. By using the analytic formulae described in Kato, Osaki (2013) (the exact formulae are described in Namekata et al. (2017)), we estimated the mass ratio of CSS J1740 to be $q = 0.077(5)$. The obtained value is very typical among WZ Sge-type dwarf novae, despite the fact that the orbital period of the system is far below the observational period minimum (Kato 2015).

However, our estimation of the mass ratio of CSS J1740 is significantly larger than that derived by Chochol et al. (2015), who obtained $q = 0.0565(20)$. This discrepancy comes from the fact that Chochol et al. (2015) used so-called Patterson relation with $\epsilon = 0.18q + 0.29q^2$, where ϵ is defined as the fractional period excess with $P_{\text{sh}}/P_{\text{orb}} - 1$ (Patterson et al. 2005). Conventionally, the mean P_{sh} was determined by using the total light curve during the plateau stage of the superoutburst, which indicates that P_{sh} is determined by combined stage A, B, and C superhumps. Recent theoretical studies suggest that stage B is the stage that the pressure effect becomes dominant, resulting in changing superhump periods (Osaki, Kato 2013b). Observationally, it is known that P_{sh} of stage A is 1.0–1.5% longer than that of stage B (Kato et al. 2009). If we determine the mean P_{sh} by using the total light curve during the plateau stage, then the estimated P_{sh} will be very close to P_{sh} during the stage B, since the most of the plateau stage consists of stage B. As a result, the mean P_{sh} may be underestimated, leading to underestimation of q

as well, as pointed out by Nakata et al. (2013). We point out that q derived by Chochol et al. (2015) may be underestimated. The exact mass ratio of CSS J1740, as well as the validity of the stage A method should be confirmed by future spectroscopic observations using a large telescope.

4 Summary

In this paper, we report on our analyses of multicolour photometry during the 2013 superoutburst of the short period dwarf nova CSS J1740. We summarize our results as follows:

- The superoutburst light curve of CSS J1740 consists of the main plateau stage, temporal dip, and long-lasting rebrightening. The light curve is classified as the type-A rebrightenings of WZ Sge-type dwarf novae.
- In the superhump modulations, there is a tendency that the superhump minima coincide with the bluest peaks of $g' - I_c$ colour variations.
- The amplitude development of superhumps is similar to other WZ Sge-type dwarf novae.
- We plot the nightly-averaged colour-colour diagram of CSS J1740 and found that the $g' - R_c$ colour indices are bluer compared with those of V455 And.
- The colour indices of the dip was significantly bluer than those of EG Cnc and WZ Sge.
- We obtained q to be 0.077(5). This value is significantly larger than that obtained by Chochol et al. (2015). We point out that Chochol et al. (2015) may underestimate q because of the usage of the conventional relation between ϵ and q .

Acknowledgments

We thank an anonymous referee for helpful comments on the manuscript of the paper. We are grateful to the Catalina Real-time Transient Survey team for making their real-time detection of transient objects available to the public. We acknowledge with thanks the variable star observations from the AAVSO and VSNET International Database contributed by observers worldwide and used in this research. We thank Dr. Tomohito Ohshima for providing us with information on the object. This work is partly supported by the Publication Committee of the National Astronomical Observatory of Japan (NAOJ). Part of this work is supported by a Research Fellowship of the Japan Society for the Promotion of Science for Young Scientists (KI).

References

- Augusteyn, T., van Kerkwijk, M. H., & van Paradijs, J. 1993, *A&A*, 267, L55
- Breedt, E., Gänsicke, B. T., Marsh, T. R., Steeghs, D., Drake, A. J., & Copperwheat, C. M. 2012, *MNRAS*, 425, 2548

- Carter, P. J., et al. 2013, MNRAS, 431, 372
- Chochol, D., et al. 2015, Acta Polytechnica CTU Proceedings, 2, 165
- Drake, A. J., et al. 2009, ApJ, 696, 870
- Fernie, J. D. 1989, PASP, 101, 225
- Gänsicke, B. T., et al. 2009, MNRAS, 397, 2170
- Gänsicke, B. T., et al. 2003, ApJ, 594, 443
- Hellier, C. 2001, Cataclysmic Variable Stars: How and why they vary (Berlin: Springer-Verlag)
- Hirose, M., & Osaki, Y. 1990, PASJ, 42, 135
- Howell, S. B., Henden, A. A., Landolt, A. U., & Dain, C. 2004, PASP, 116, 527
- Howell, S. B., Szkody, P., & Cannizzo, J. K. 1995, ApJ, 439, 337
- Imada, A., Isogai, K., Araki, T., Tanada, S., Yanagisawa, K., & Kawai, N. 2018, PASJ, 70, 2
- Imada, A., Kubota, K., Kato, T., Nogami, D., Maehara, H., Nakajima, K., Uemura, M., & Ishioka, R. 2006, PASJ, 58, L23
- Ishioka, R., et al. 2001, PASJ, 53, 905
- Isogai, M., Arai, A., Yonehara, A., Kawakita, H., Uemura, M., & Nogami, D. 2015, PASJ, 67, 7
- Kato, T. 2002, PASJ, 54, L11
- Kato, T. 2015, PASJ, 67, 108
- Kato, T., et al. 2015, PASJ, 67, 105
- Kato, T., et al. 2009, PASJ, 61, S395
- Kato, T., et al. 2010, PASJ, 62, 1525
- Kato, T., Nogami, D., Matsumoto, K., & Baba, H. 2004a, PASJ, 56, S109
- Kato, T., & Osaki, Y. 2013, PASJ, 65, 115
- Kato, T., Sekine, Y., & Hirata, R. 2001, PASJ, 53, 1191
- Kato, T., Uemura, M., Ishioka, R., Nogami, D., Kunjaya, C., Baba, H., & Yamaoka, H. 2004b, PASJ, 56, S1
- Kennedy, M., Garnavich, P., Callanan, P., Szkody, P., Littlefield, C., & Pogge, R. 2015, ApJ, 815, 131
- Kimura, M., et al. 2016a, Nature, 529, 54
- Kimura, M., et al. 2016b, PASJ, 68, L2
- Knigge, C., Baraffe, I., & Patterson, J. 2011, ApJs, 194, 28
- Kotani, T., et al. 2005, Nuovo Cimento C Geophysics Space Physics C, 28, 755
- Lasota, J.-P. 2001, New Astron. Reviews, 45, 449
- Littlefair, S. P., Dhillon, V. S., Marsh, T. R., Gänsicke, B. T., Baraffe, I., & Watson, C. A. 2007, MNRAS, 381, 827
- Littlefield, C., et al. 2013, AJ, 145, 145
- Matsui, R., et al. 2009, PASJ, 61, 1081
- Meyer, F., & Meyer-Hofmeister, E. 1981, A&A, 104, L10
- Nakagawa, S., Noguchi, R., Iino, E., Ogura, K., Matsumoto, K., Arai, A., Isogai, M., & Uemura, M. 2013, PASJ, 65, 70
- Nakata, C., et al. 2013, PASJ, 65, 117
- Namekata, K., et al. 2017, PASJ, 69, 2
- Neustroev, V. V., et al. 2017, MNRAS, 467, 597
- Nogami, D., Kato, T., Baba, H., Matsumoto, K., Arimoto, J., Tanabe, K., & Ishikawa, K. 1997, ApJ, 490, 840
- Okyudo, M., Kato, T., Ishida, T., Tokimasa, N., & Yamaoka, H. 1993, PASJ, 45, L63
- Olech, A. 1997, Acta Astron., 47, 281
- Osaki, Y. 1989, PASJ, 41, 1005
- Osaki, Y. 1996, PASP, 108, 39
- Osaki, Y., & Kato, T. 2013a, PASJ, 65, 50
- Osaki, Y., & Kato, T. 2013b, PASJ, 65, 95
- Osaki, Y., & Meyer, F. 2002, A&A, 383, 574
- Patterson, J., et al. 2005, PASP, 117, 1204
- Patterson, J., et al. 1998, PASP, 110, 1290
- Patterson, J., et al. 2002, PASP, 114, 721
- Patterson, J., Thorstensen, J. R., & Knigge, C. 2008, PASP, 120, 510
- Podsiadlowski, Ph., Han, Z., & Rappaport, S. 2003, MNRAS, 340, 1214
- Prieto, J. L., et al. 2013, Astronomer's Telegram, 4999
- Shappee, B. J., et al. 2014, ApJ, 788, 48
- Smak, J. 1984, Acta Astron., 34, 161
- Smith, J. A., et al. 2002, AJ, 123, 2121
- Stellingwerf, R. F. 1978, ApJ, 224, 953
- Szkody, P., et al. 2005, AJ, 129, 2386
- Thorstensen, J. R., Fenton, W. H., Patterson, J. O., Kemp, J., Krajci, T., & Baraffe, I. 2002, ApJ, 567, L49
- Uemura, M., et al. 2008, PASJ, 60, 227
- Uemura, M., et al. 2003, Nature, 423, 843
- Uemura, M., et al. 2002, PASJ, 54, 599
- Uemura, M., Kato, T., Nogami, D., & Ohsugi, T. 2010, PASJ, 62, 613
- Warner, B. 1995, Cataclysmic Variable Stars (Cambridge: Cambridge University Press)
- Wei, J.-Y., Jiang, X.-J., Xu, D.-W., Zhou, A.-Y., & Hu, J.-Y. 2001, Chin. J. Astron. Astrophys., 1, 483
- Whitehurst, R. 1988, MNRAS, 232, 35

Table 2. Timings of superhump maxima.

E	Max*	Error	O - C [†]	N [‡]	Source§	E	Max*	Error	O - C [†]	N [‡]	Source§
0	56407.6657	0.0010	-0.0257	80	A	156	56414.7972	0.0005	0.0001	54	A
1	56407.7103	0.0013	-0.0267	79	A	170	56415.4335	0.0002	-0.0012	90	A
21	56408.6441	0.0006	-0.0038	112	A	171	56415.4791	0.0003	-0.0012	87	A
22	56408.6889	0.0004	-0.0046	158	A	172	56415.5252	0.0005	-0.0006	69	A
23	56408.7329	0.0003	-0.0061	154	A	184	56416.0714	0.0008	-0.0010	79	M
24	56408.7805	0.0003	-0.0040	156	A	186	56416.1633	0.0013	-0.0003	45	M
29	56409.0122	0.0012	-0.0001	77	M	187	56416.2081	0.0007	-0.0010	76	M
30	56409.0580	0.0006	0.0002	82	M	206	56417.0726	0.0008	-0.0020	77	M
31	56409.1048	0.0005	0.0014	82	M	230	56418.1665	0.0006	-0.0012	63	M
32	56409.1513	0.0005	0.0023	81	M	231	56418.2112	0.0006	-0.0020	76	M
33	56409.1996	0.0005	0.0051	80	M	237	56418.4863	0.0004	-0.0003	83	A
42	56409.6126	0.0004	0.0082	61	A	238	56418.5302	0.0004	-0.0019	89	A
43	56409.6573	0.0004	0.0073	79	A	250	56419.0756	0.0008	-0.0031	76	M
44	56409.7022	0.0002	0.0066	78	A	251	56419.1230	0.0011	-0.0013	75	M
45	56409.7483	0.0002	0.0072	79	A	252	56419.1672	0.0007	-0.0026	80	M
46	56409.7933	0.0002	0.0066	77	A	253	56419.2125	0.0009	-0.0029	78	M
60	56410.4319	0.0002	0.0076	87	A	259	56419.4859	0.0005	-0.0028	85	A
61	56410.4771	0.0002	0.0072	87	A	260	56419.5321	0.0004	-0.0021	81	A
84	56411.5232	0.0002	0.0057	87	A	261	56419.5766	0.0003	-0.0032	88	A
85	56411.5690	0.0002	0.0059	82	A	262	56419.6236	0.0004	-0.0017	65	A
86	56411.6141	0.0002	0.0055	90	A	265	56419.7604	0.0004	-0.0016	73	A
105	56412.4777	0.0002	0.0036	87	A	266	56419.8060	0.0004	-0.0016	76	A
106	56412.5236	0.0002	0.0040	89	A	267	56419.8506	0.0004	-0.0025	76	A
107	56412.5688	0.0002	0.0036	92	A	268	56419.8955	0.0004	-0.0031	77	A
108	56412.6147	0.0002	0.0040	91	A	269	56419.9420	0.0005	-0.0021	74	A
122	56413.2504	0.0006	0.0020	82	M	270	56419.9883	0.0007	-0.0014	77	A
127	56413.4776	0.0002	0.0014	89	A	273	56420.1258	0.0006	-0.0005	74	M
128	56413.5231	0.0002	0.0014	91	A	274	56420.1689	0.0008	-0.0031	80	M
129	56413.5681	0.0002	0.0009	86	A	275	56420.2176	0.0007	0.0001	76	M
130	56413.6140	0.0003	0.0012	151	A	294	56421.0838	0.0008	0.0009	70	M
131	56413.6591	0.0007	0.0008	80	A	295	56421.1292	0.0010	0.0008	77	M
132	56413.7045	0.0003	0.0006	79	A	296	56421.1743	0.0007	0.0003	76	M
133	56413.7508	0.0003	0.0013	79	A	316	56422.0849	0.0019	-0.0001	69	M
141	56414.1137	0.0003	-0.0001	162	M	368	56424.4587	0.0004	0.0052	168	A
142	56414.1604	0.0003	0.0010	156	M	369	56424.5038	0.0005	0.0047	164	A
143	56414.2050	0.0003	0.0001	134	M	370	56424.5516	0.0005	0.0070	166	A
148	56414.4330	0.0003	0.0003	85	A	382	56425.1005	0.0014	0.0093	75	M
149	56414.4783	0.0002	0.0001	88	A	384	56425.1856	0.0010	0.0033	77	M
150	56414.5234	0.0003	-0.0004	91	A	385	56425.2348	0.0033	0.0069	78	M
151	56414.5687	0.0002	-0.0006	89	A	470	56429.0909	0.0013	-0.0087	78	M
152	56414.6144	0.0003	-0.0005	161	A	471	56429.1432	0.0025	-0.0019	81	M
153	56414.6598	0.0004	-0.0006	79	A	479	56429.5033	0.0029	-0.0062	49	A
154	56414.7048	0.0003	-0.0012	80	A	480	56429.5539	0.0018	-0.0012	49	A
155	56414.7512	0.0004	-0.0003	77	A						

*BJD-2400000.

[†]Against max = 2456407.6914 + 0.045549 E[‡]Total datapoints used to determine the maximum.

§A:AAVSO M:MITSuME.

Table 3. Values of the phase difference between superhumps and colour variations.

Object	Stage A	Stage B	References
CSS J1740	0.5	0.3	this work
V455 And	-	0.15	1
EZ Lyn	-	0.3-0.5	2
SSS J1222	0.3	0.5	3
HV Vir	0.4	0.5	4
OT J0120	0.5	0.2	4

SSS J1222 = SSS J122221.7–311525.

OT J0120 = OT J012059.6+325545.

1:Matsui et al. (2009).

2:Isogai et al. (2015).

3:Neustroev et al. (2017).

4:Imada et al. (2018).

Table 4. $g' - R_c$ and $R_c - I_c$ colours during the dips.

Object	$g' - R_c$	$R_c - I_c$	References
CSS J1740	0.02	0.20	this work
EG Cnc	0.49	0.40	1
WZ Sge	0.41	0.33	2

1:Patterson et al. (1998). 2:Howell et al. (2004)